Biosensors and Bioelectronics 49 (2013) 387–393

Contents lists available at SciVerse ScienceDirect

Biosensors and Bioelectronics

journal homepage: www.elsevier.com/locate/bios

Oriented antibody immobilization by site-specific UV photocrosslinking of biotin at the conserved nucleotide binding site for enhanced antigen detection

Nathan J. Alves [a], Nur Mustafaoglu [a], Basar Bilgicer [a,b,c,*]

[a] Department of Chemical and Biomolecular Engineering, University of Notre Dame, Notre Dame, IN 46556, USA
[b] Advanced Diagnostics and Therapeutics, University of Notre Dame, Notre Dame, IN 46556, USA
[c] Department of Chemistry and Biochemistry, University of Notre Dame, Notre Dame, IN 46556, USA

ARTICLE INFO

Article history:
Received 28 March 2013
Received in revised form
29 May 2013
Accepted 30 May 2013
Available online 6 June 2013

Keywords:
Biosensor
Immunoglobulin
Site-specific crosslinking
Oriented immobilization
ELISA

ABSTRACT

The nucleotide binding site (NBS) is an under-utilized, highly conserved binding site found within the variable region of nearly all antibody Fab arms. Here, we describe an NBS specific UV photocrosslinking biotinylation method (UV-NBS^{Biotin}) for the oriented immobilization of antibodies to streptavidin-coated surfaces, such that the antigen binding activity remains unaffected. An optimal UV exposure of 1 J/cm^2 yielded an average conjugation efficiency of ~1 biotin per antibody resulting in significant immobilization efficiency while maintaining maximal antigen binding activity. With the continued push for miniaturization of medical diagnostics to reduce cost and increase patient accessibility the ever shrinking on chip detection areas necessitate the highest level of immobilized antibody activity to maximize assay detection capabilities. The UV-NBS^{Biotin} method yielded surfaces with significantly enhanced antigen detection capabilities, improved antigen detection sensitivity and the highest amount of active surface immobilized antibody when compared to other common immobilization methods including: ε-NH_3^+ surface conjugation, NHS–Biotin, and direct physical adsorption. Taken together, the UV-NBS^{Biotin} method provides a universal, site-specific immobilization method that is amenable to any available assay detection modality with potential significant implications in the development of miniaturized medical diagnostics and lab on a chip technologies.

1. Introduction

The nucleotide binding site (NBS) is an under-utilized, highly conserved binding site found within the variable region of nearly all antibody Fab arms. This paper describes a method for the oriented immobilization of antibodies to streptavidin coated surfaces by the site-specific UV photocrosslinking of biotin to antibody NBS, such that the antigen binding activity is preserved. Antibodies are often utilized as surface immobilized capture proteins for many immunosensor-based applications including screening of pathogens, disease detection, point-of-care clinical analysis and various medical diagnostics (Caygill et al., 2010; Leonard et al., 2003; Liu et al., 2008; Warsinke, 2009). The oriented immobilization of antibodies to surfaces is particularly critical when antibodies are utilized as detection molecules in microfluidic based miniaturized medical diagnostics and for microarray applications. Medical diagnostics utilizing micro and nanofluidic channels are becoming more prevalent and allowing for increased patient accessibility and reduced cost through miniaturization (Kim et al., 2012; Hu and Li, 2011; Mohammed and Desmulliez, 2011; Ng et al., 2010). The significantly reduced on chip detection areas necessitate the highest level of antibody activity to ensure that each immobilized antibody is capable of binding antigen to provide for improved assay detection capabilities.

The current standard methods of immobilizing antibodies to surfaces involve either non-covalent physical adsorption to detection surfaces through nonspecific hydrophobic interactions (physical adsorption method) or through covalent modification of lysine side chain amino groups present throughout the antibody surface (Ghani et al., 2011; Li et al., 2008; Moelans et al., 2011; Shephard, 2008; Xiong and Ge, 2011; Yotsumoto, 2008). Conjugation to these amino groups is commonly carried out with N-hydroxysuccinimide (NHS) activated affinity tags, such as NHS–Biotin to immobilize to streptavidin coated surfaces, or through direct reaction of antibody amino groups to amine reactive surfaces (ε-NH_3^+ method) (Byeon et al., 2010; Faye et al., 2012; MacBeath

* Corresponding author at: Department of Chemical and Biomolecular Engineering, Department of Chemistry and Biochemistry, University of Notre Dame, 165 Fitzpatrick Hall, Notre Dame, IN 46556-5637, United States. Tel.: +1 574 631 1429; fax: +1 574 631 8366.
E-mail address: bbilgicer@nd.edu (B. Bilgicer).

0956-5663/$ - see front matter © 2013 Elsevier B.V. All rights reserved.
http://dx.doi.org/10.1016/j.bios.2013.05.052

and Schreiber, 2000; Mendoza et al., 1999; Patel et al., 1997). These methods, however, result in disordered antibody molecules on the detection surface and yield $<10\%$ active antibody due to steric blocking of antigen binding sites on the heterogeneous antibody coated surface (Butler et al., 1992, 1993; Kausaite-Minkstimiene et al., 2010; Peluso et al., 2003; Vijayendran and Leckband, 2001). Despite resulting in a significant loss of antibody activity, these methods remain the most commonly implemented methods of antigen detection due to their simplicity of execution and availability of common reagents.

While there are a few available site-specific antibody immobilization methods, these are often associated with either complicated chemical procedures, or the conjugation conditions are detrimental to antibody activity (Kausaite-Minkstimiene et al., 2010; Peluso et al., 2003; Vijayendran and Leckband, 2001). One of the most common site-specific immobilization methods is selective reduction of the disulfide bonds between antibody heavy chains, making the cysteine side chains accessible as reactive sites (Brogan et al., 2003; Lee et al., 2005; Vikholm-Lundin, 2005). Another common method is selective oxidation of antibody carbohydrate chains to form reactive aldehyde groups that can be used to selectively couple to hydrazine functionalized surfaces (Hoffman and Oshannessy, 1988; Quarles, 1985; Zara et al., 1991). These coupling techniques can have variable outcomes from antibody to antibody and often result in reduced antibody activity through reduction of Fab disulfide bonds or over exposure to oxidative chemicals, respectively (Kausaite-Minkstimiene et al., 2010; Peluso et al., 2003; Vijayendran and Leckband, 2001). When immobilizing an antibody, maintaining its antigen binding activity is a critical factor that directly effects device fabrication reproducibility, assay sensitivity, and dynamic range of antigen detection (Trilling et al., 2013). Therefore, further advances in site-specific antibody immobilization techniques that provide a practical and reproducible method of immobilization, while maintaining antigen binding activity, are necessary.

In a previous report, we addressed this need by developing a UV-NBS immobilization method that allowed for the oriented immobilization of antibodies at their NBS through UV photocrosslinking to NBS–ligand conjugated surfaces (Alves et al., 2012). The UV-NBS functionalized surfaces resulted in increased antigen detection capabilities and increased assay sensitivity compared to other standard immobilization methods despite the overall lower antibody immobilization efficiency. Here we describe an alternate photochemistry based NBS-specific antibody immobilization method that utilizes biotin for oriented immobilization to streptavidin-functionalized surfaces (UV-NBS^{Biotin}, Fig. 1). We predicted that site-specifically conjugating a biotin molecule to the antibody NBS prior to immobilization would allow for nearly 100% antibody functionalization to overcome the poor immobilization efficiency of the previously reported UV-NBS method while still maintaining maximum antibody activity. In earlier publications, we also extensively characterized the NBS using molecular modeling, and showed that it is a highly conserved binding pocket located in the conserved region between the variable light (V_L) and variable heavy (V_H) domain of all antibody isotypes (Handlogten et al., 2011; Rajagopalan et al., 1996). Through an *in silico* docking study, indole-3-butryic acid (IBA) was selected as a high binding NBS-ligand, with experimental K_d values ranging between 1 and 8 μM, depending on the antibody (Handlogten et al., 2011). The NBS is comprised of amino acid residues with aromatic side chains [Y/F42 and Y/F103 within the V_L; Y103 and W118 within the V_H] (Lefranc et al., 2003) that when exposed to UV light (254 nm) form reactive radicals that covalently crosslink to other aromatic moieties (Meisenheimer and Koch, 1997; Alves et al., 2013). Therefore, the NBS provides a useful site for selective conjugation of antibodies to small molecule ligands that contain aromatic rings, such as IBA, which was selected for the application described in this study.

To demonstrate the utility of the UV-NBS^{Biotin} immobilization method, a prostate specific antigen (PSA) detection system was selected to assess the antibody immobilization efficiency, antigen detection sensitivity, limit of detection (LOD) and the dynamic range of antigen detection. PSA, also known as kallikrein-3, is a 30–34 kDa glycoprotein enzyme whose serum levels have been implicated in the early detection of prostate cancer (Sutcliffe et al., 2012). While PSA screening is no longer recommended by the United States Preventative Services Task Force based on its limited aid in the reduction of prostate related mortality, the model system still provides important validation of new immobilization techniques applied to diagnostic assays (Moyer and US Preventive Serv Task Force, 2012; Sutcliffe et al., 2012). A mouse IgG PSA-specific capture antibody (IgG^{PSA}, K_d≤4 pM) (Washburn et al., 2011), free PSA, and PSA detection antibody (det-IgG^{PSA}) were selected to demonstrate the advantages of the UV-NBS^{Biotin} oriented immobilization method compared to ε-NH_3^+ and physical adsorption immobilization techniques.

2. Materials and methods

2.1. Materials

IBA, Biotin N-hydroxysuccinimide ester (NHS–Biotin), N,N-Diisopropylethylamine (DIEA), were purchased from Sigma-Aldrich (St. Louis, MO). Streptavidin–HRP and HRP-conjugated IgG Fcγ specific goat anti-mouse were purchased from Jackson ImmunoResearch

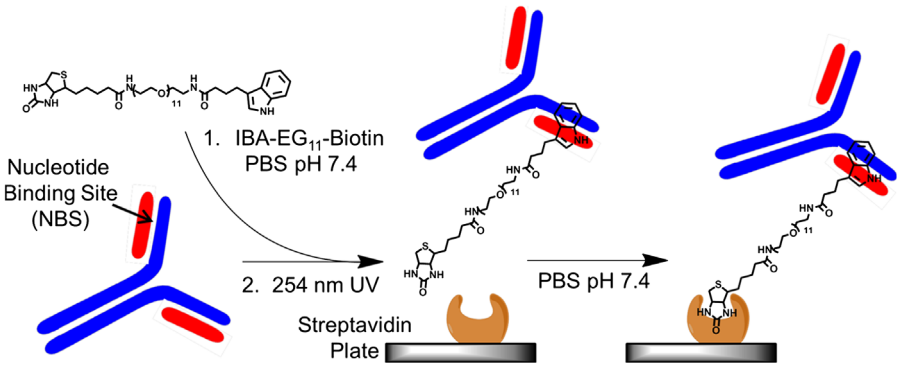

Fig. 1. Schematic representation of the UV-NBS^{Biotin} immobilization method. Antibodies associate with IBA–EG_{11}–Biotin ligand at the NBS, and upon UV exposure a covalent bond forms between IBA and the antibody. The IBA–EG_{11}–Biotin functionalized antibody then binds to a streptavidin functionalized plate, tethering the antibody to the surface. The oriented, site-specific conjugation of the antibody through its NBS preserves antibody's antigen binding activity.

(West Grove, PA). Heat shock isolated bovine serum albumin (BSA), Amicon Ultra centrifugal filters (0.5 mL, 10 K) and Coomassie R-250 were purchased from EMD Millipore (Billerica, MA). Amplex Red Assay Kit was purchased from Invitrogen (Grand Island, NY). Maleic anhydride amine reactive 96-well plates and streptavidin coated 96-well plates were purchased from Thermo Scientific (Rockford, IL). NovaPEG Rink Amide resin, and all other amino acids were purchased from Novabiochem (Billerica, MA). Fmoc-N-amido-dPEG$_2$-acid was purchased from Quanta Biodesign (Powell, OH). Tris–gly running buffer, transfer buffer, and tris buffered saline (TBS) were purchased from Boston Bioproducts (Ashland, MA). Mouse anti-PSA (IgG^{PSA} capture antibody, clone: B731M), mouse anti-PSA (det-IgG^{PSA} detection antibody, clone: 5A6) and purified free prostate specific antigen (PSA) were purchased from Meridian Life Science, Inc. (Memphis, TN).

2.2. Photocrosslinking of IBA-conjugated ligands (IBA-ligand) to antibodies

All antibodies undergoing photocrosslinking were purchased as purified antibodies with no protein stabilizers. Sodium azide, a very UV reactive preservative, and other small molecule additives were removed prior to UV exposure via membrane filtration. Antibodies were incubated with the IBA-ligands for 1 h prior to UV exposure at room temperature (RT). Control over the UV energies delivered to the samples was achieved using a Spectroline UV Select Series Crosslinker from Spectronics at a wavelength of 254 nm.

2.3. Synthesis of IBA–EG$_{11}$–Biotin

The IBA–EG$_{11}$-amine ligand was synthesized by coupling IBA to mono-N-t-boc-amido-dPEG$_{11}$-amine following HBTU activation in DMF and DIEA at RT for 3.5 h while agitating. After rotate evaporating DMF, the t-boc protecting group was removed in a solution of 4% triisopropylsilane, 4% D.I. water, and 92% trifluoroacetic acid (TFA) for 45 min at RT. IBA–EG$_{11}$-amine was purified via RP-HPLC on a Zorbax C18 column, and characterized using MALDI-TOF MS. The calculated exact mass for the IBA–EG$_{11}$-amine ($C_{36}H_{63}N_3O_{12}$) was 729.44 Da; found 730.49 Da. Biotin was then conjugated to the purified IBA-EG$_{11}$-amine to synthesize IBA–EG$_{11}$–Biotin which was also purified via RP-HPLC on a Zorbax C18 column (Fig. S1 in Supporting information). The yield 70%, and product purity was confirmed using RP-HPLC on an analytical Zorbax C18 column to be $>95\%$.

2.4. Synthesis of IBA–FITC

IBA–FITC was synthesized by HBTU activation of IBA in DMF mixed in equimolar amounts of FITC and L-Lysine. The reaction was carried out overnight while shaking, purified via RP-HPLC on a Zorbax C18 column, and characterized using MALDI-TOF MS (Fig. S2 in Supporting information). The yield was 75%, and product purity was confirmed using RP-HPLC on an analytical Zorbax C18 column to be $>95\%$.

2.5. Assessing antigen binding activity, Fc stability, and biotinylation of the antibody via ELISA

Antigen coated ELISA plates were generated by adsorbing PSA (10 nM or 0.34 mg/mL) to high binding 96-well ELISA plates in 0.05 M carbonate–bicarbonate coating buffer at pH 9.6 for 2 h at RT. The plates were washed to remove any unbound components using an automated plate washer with three cycles of 200 μL PBS with 0.05% Tween 20 at pH 7.4 (MDS Aquamax 2000). All plate surfaces were then blocked with BSA blocking buffer (200 μL of 5% BSA in PBS pH 7.4 with 0.1% Tween 20) for 1 h. *Antigen binding activity and Fc stability*: The IgG^{PSA} capture antibody was exposed to UV in the presence or absence of 300 μM IBA–EG$_{11}$–Biotin and was then incubated on the antigen coated plates. The wells were then incubated with a 1:5000 dilution of HRP–anti-Fc antibody (1.0 mg/mL stock) in BSA blocking buffer for 1 h to quantify the total amount of antigen bound antibody (active Fc). *IgG^{PSA} Biotinylation*: To assess the degree of UV biotinylation for each sample, the antigen bound IBA–EG$_{11}$–Biotin UV exposed IgG^{PSA} antibody wells were incubated with a 1:10,000 dilution of streptavidin–HRP (1.0 mg/mL stock) in BSA blocking buffer for 1 h. Amplex red, the HRP substrate, was added and fluorescent product formation was observed on a Molecular Devices SpectraMax M5 plate reader (ex. 570 nm, em. 592 nm) for all ELISA assays. Control experiments performed without IBA–EG$_{11}$–Biotin were used as background for the biotinylation detection measurements. The results are reported as relative fluorescence units (RFU). All data represents means ($\pm$SD) of triplicate experiments.

2.6. Determination of average number of UV Conjugations via size exclusion chromatography (SEC)

A Tosoh Biosciences G4000SW$_{XL}$ (7.8 mm ID $\times$ 30 cm) size exclusion column was used to assess the average number of IBA–FITC conjugations to the antibody over a range of UV energies (0–1.5 J/cm^2). Antibody samples were prepared as indicated, and 20 μL of each sample were analyzed on the SEC column. Each SEC run was achieved using a 25 min isocratic gradient of 50 mM PBS at pH 6.8 with 370 mM NaCl and 0.1% Tween 20. All samples were analyzed at 220 and 280 nm to detect antibody content and at 494 nm to detect covalently bound IBA–FITC. Each absorbance spectrum was integrated on Chemstation LC software and used to calculate total antibody content and total nmoles of covalently bound IBA–FITC compared to a calibration curve ($y=836.94x$, $R^2=0.9876$). The nmoles of FITC divided by the nmoles of antibody gives the average number of IBA–FITC conjugations per antibody.

2.7. Western blot analysis for determination of the photocrosslinking site

IgG^{PSA}, at 20 μM, was incubated with excess IBA–EG$_{11}$–Biotin (300 μM) in PBS buffer at pH 7.4 and exposed to the indicated amount of UV energy (0–1.5 J/cm^2). The samples were run on a 10% SDS-PAGE gel with a tris–glycine running buffer under reducing conditions at 110 V for 1 h and were transferred to a nitrocellulose membrane at 110 V for 90 min in a 10% MeOH transfer buffer. The membrane was blocked with 10% dry milk in TBS for 1 h and was then blotted with 1:10,000 dilution of streptavidin–HRP for 1 h at RT. A chemiluminescent HRP substrate was used to detect the location where IBA–EG$_{11}$–Biotin was covalently conjugated to the antibody. The SDS-PAGE gel was coomassie blue stained in a solution of 10% acetic acid, 20% methanol, 0.15% Coomassie R-250 for 30 min and destained in a solution of 20% acetic acid, 20% methanol, 60% D.I. water for 1.5 h. Control experiments performed in the absence of UV exposure, or in the absence of IBA–EG$_{11}$–Biotin did not yield any detectable bands.

2.8. UV-NBS^{Biotin} antibody immobilization method

IgG^{PSA} incubated with 300 μM IBA–EG$_{11}$–Biotin in PBS was exposed to 1 J/cm^2 of UV energy. The unbound IBA–EG$_{11}$–Biotin was removed via membrane filtration. The purified, biotinylated IgG^{PSA} was then incubated on streptavidin coated ELISA plates in BSA blocking buffer for 2 h at RT. In all cases, unbound antibody was then washed using an automated plate washer. Antibody

immobilized wells were then blocked with BSA blocking buffer for 1 h to prevent non-specific adhesion/interactions.

2.9. Non site-specific immobilization methods

Physical adsorption immobilization method: was carried out by incubating antibody on high bind ELISA plate surfaces in 0.05 M carbonate-bicarbonate coating buffer at pH 9.6 for 2 h at RT. *ε-NH_3^+immobilization method:* lysine side-chains present on the antibody surface were reacted to amine reactive maleic anhydride 96-well plates for 2 h at RT in PBS buffer at pH 8.0. Any remaining reactive sites were then quenched with 50 mM Tris buffer with 100 mM NaCl at pH 8.0 for 1 h. *NHS–Biotin immobilization method*: antibody was biotinylated with NHS–Biotin following the manufacturer suggested protocol and unreacted NHS–Biotin was removed via membrane filtration prior to incubation on streptavidin coated plate surfaces in BSA blocking buffer for 2 h at RT. All surfaces were then washed and blocked using BSA blocking buffer for 1 h.

2.10. Determination of total antibody content of antibody immobilized surfaces

Quantification of the total surface immobilized antibody for each of the four immobilization techniques with initial antibody amounts of 0–50 fmole (0–0.5 nM) were performed using an HRP conjugated Fc-specific secondary antibody from goat at a 1:5000 dilution (1.0 mg/mL stock) in BSA blocking buffer for 1 h. Amplex red was used as the enzymatic substrate and the results are reported as RFU. The resulting antibody immobilization signal at different starting antibody amounts was fit by linear regression. The slope of the linear regression line was determined to be the antibody immobilization efficiency for each of the immobilization methods. Control experiments performed without immobilized antibody were used as background.

2.11. Determination of antigen detection capabilities, assay sensitivity and limit of detection

The antigen detection capabilities for all four immobilization methods were determined by ELISA. Briefly, IgG^{PSA} immobilized surfaces (1 or 5 fmole, 0.01 or 0.05 nM, of initial antibody) were incubated with PSA (0–1000 fmole or 0–10 nM) in 100 μL of BSA blocking buffer for 1.5 h. Unbound PSA was washed and the wells were incubated with a 1:2500 dilution of det-IgG^{PSA} (5A6, 1.0 mg/mL stock) in BSA blocking buffer for 1 h. An Fc-specific HRP conjugated antibody (1:2500 dilution) was then used to detect the presence of the IgG^{PSA} detection antibody bound to PSA. Amplex red was then added and fluorescent product formation was observed, results are reported as RFU. The resulting antigen detection signal vs. amount of antigen plots were fit by natural log regression. Sensitivity was determined from the coefficient of the natural log multiplier from the regression line. The limit of detection (LOD) for each immobilization method was determined to be the antigen concentration at 3 standard deviations to the mean of the zero PSA standard. Control experiments performed without PSA, and without detection antibody were used as background for the antigen detection measurements.

3. Results and discussion

3.1. Effect of UV energy on antibody binding activity and Fc recognition

We first evaluated the effect of increasing UV energies on IBA photocrosslinking to the antibody by using IBA–EG_{11}–Biotin via an ELISA assay (Supporting information Fig. S1). UV exposure initiates the site-specific photocrosslinking of the IBA-ligand to the antibody NBS but can potentially have damaging effects to the antigen recognition site as well as Fc structure. For this reason, the effects of UV exposure to the IgG^{PSA} were evaluated to ensure antibody activity was preserved at the UV exposures necessary to utilize the UV-NBS^{Biotin} method. IgG^{PSA} was exposed to increasing UV energies (0–5 J/cm^2) in the presence and absence of a saturating concentration of IBA–EG_{11}–Biotin (300 μM) in PBS pH 7.4 (Supporting information Fig. S3). PSA was directly immobilized onto high binding ELISA plates through physical adsorption. The UV-exposed IgG^{PSA} was then incubated on the plate surface and allowed to bind to PSA. Both antigen recognition and Fc stability were assessed simultaneously by binding of an HRP conjugated Fc-specific secondary antibody, evaluating the total amount of antigen-bound antibody at increasing UV energies. In this assay, a reduction in the signal intensity at high UV energies is indicative of damage to either the antigen binding sites preventing IgG^{PSA} from binding its surface immobilized antigen or damage to the Fc region preventing detection by the Fc-specific HRP conjugated secondary antibody. Our results demonstrated nearly no observable reduction in antibody antigen binding activity or Fc recognition up to UV energies of 2.0 J/cm^2, with a slight increase in UV damage to the antibody in the absence of IBA–EG_{11}–Biotin (Fig. 2A). This result was expected since the presence of IBA–EG_{11}–Biotin in solution effectively screens the antibody from full exposure by partially adsorbing the UV energy. These results demonstrate that UV energies < 2.0 J/cm^2 can be utilized during the UV-NBS^{Biotin} immobilization of IgG^{PSA} as there is minimal impact on both antigen binding activity and recognition of the antibody Fc by secondary antibodies at these UV energies.

3.2. Determination of the optimal UV energy for IBA–EG_{11}–Biotin photocrosslinking

To determine the photocrosslinking efficiency of IBA–EG_{11}–Biotin to IgG^{PSA}, photocrosslinked antibody was incubated on plates coated with antigen and the degree of antibody biotinylation was determined by quantifying streptavidin–HRP binding. IBA–EG_{11}–Biotin photocrosslinking efficiency increased with increasing UV energy, with a maximum antibody biotinylation occurring between 1.0 and 2.0 J/cm^2 (Fig. 2B). A plateau in antibody biotinylation was observed that is indicative of a specific conjugation site becoming saturated. Since this assay did not depend upon Fc recognition for detection of antigen bound antibody it was determined that UV damage at the antibody antigen recognition sites, inhibiting antibody binding to the surface, was the main contributor to the decline in the biotinylation signal intensity at UV energies > 2.0 J/cm^2. Based on the results presented in these two ELISA assays (Fig. 2A, B) we determined 0.5–1.5 J/cm^2 to be an effective UV exposure range that can be used for the efficient photocrosslinking of IBA–EG_{11}–Biotin to IgG^{PSA}, without reducing antigen binding or Fc activity. This UV range was consistent with our previous results (Alves et al., 2012, Alves et al., 2013).

3.3. Effect of UV energy on the number of conjugations per antibody

When utilizing the UV-NBS photocrosslinking method we anticipate a maximum of two IBA-ligand conjugations per antibody as there are two NBS per antibody. IBA–FITC was selected to quantify the average number of conjugations per antibody (Supporting information Fig. S3). FITC was selected as it has a maximum absorbance (494 nm) well outside the range of typical protein adsorption (220 and 280 nm) allowing for accurate quantitation of the number of conjugations. IgG^{PSA} was exposed to increasing UV energies in the presence of saturating levels of

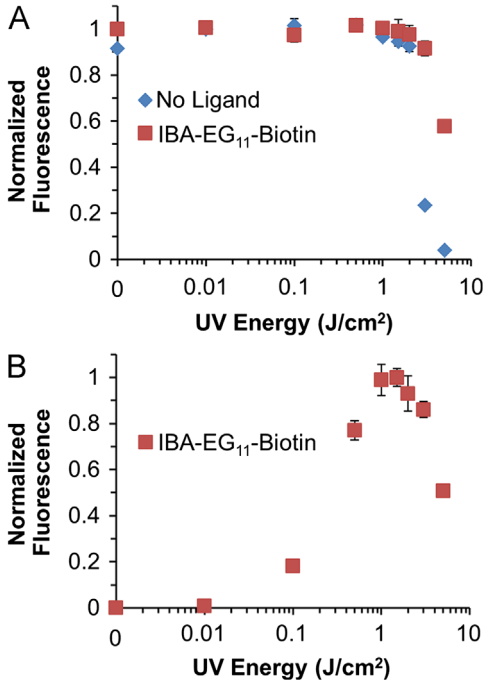

Fig. 2. The effects of UV energy exposure on antigen binding activity, Fc recognition and biotinylation efficiency as determined by ELISA assays. (A) UV exposed IgG^{PSA}, in the presence or absence of 300 μM IBA–EG_{11}–Biotin, was allowed to bind to surface immobilized PSA and the total amount of bound antibody was detected using an Fc-specific, HRP conjugated antibody. (B) Photocrosslinking efficiency of IBA–EG_{11}–Biotin to the antibody at the NBS was determined by an indirect ELISA assay, where the total biotinylation levels of IgG^{PSA} were detected by streptavidin–HRP after binding to surface immobilized PSA. All data represents means (±SD) of triplicate experiments.

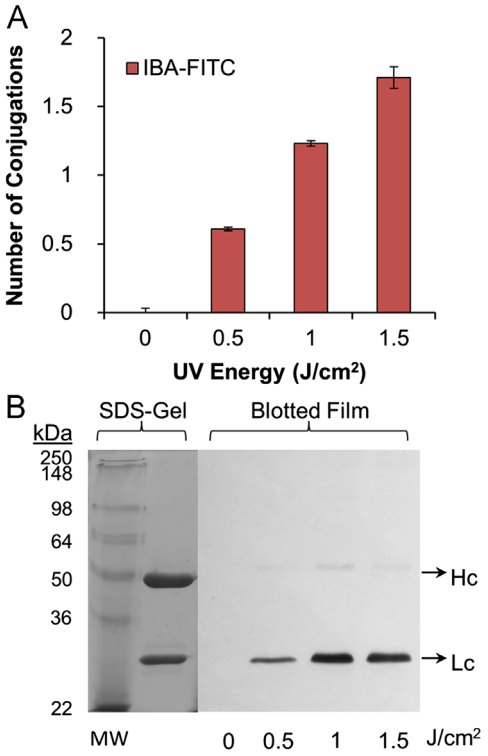

Fig. 3. The effect of UV energy on the average number, and location, of IBA–FITC conjugations per antibody. (A) Number of conjugations was determined from absorbance at 494 nm SEC peak integrations at fixed ligand and antibody concentrations of 300 μM and 20 μM, respectively. All data represents means (±SD) of triplicate experiments. (B) Western blot analysis of UV-NBS photocrosslinking site on IgG^{PSA}. IBA–EG_{11}–Biotin was photocrosslinked to the antibody by exposure to UV energy from 0 to 1.5 J/cm^2 in PBS buffer. SDS-PAGE was run under reducing conditions and the proteins were transferred to a nitrocellulose membrane. The SDS-PAGE gel was stained by coomassie blue. Streptavidin–HRP was used to probe for covalently conjugated IBA–EG_{11}–Biotin. Blotted film shows that biotin tag only appears on the antibody light chain.

IBA–FITC (300 μM), providing for complete non-covalent association of IBA–FITC to all NBS prior to UV exposure (Fig. 3A). The IBA–FITC conjugated antibody was then injected on a size exclusion column to effectively separate non-conjugated IBA–FITC ligand from the conjugated antibody. By integrating the 494, 220 and 280 nm elution profiles and correlating the values to molar calibration curves, the average number of IBA–FITC conjugations per antibody was calculated by dividing nmoles of FITC by nmoles of antibody injected on the column (Fig. 3A). Increasing UV energy resulted in an increase in the number of conjugations, reaching a maximum of 1.71 conjugations per antibody at 1.5 J/cm^2 UV exposure. For maximum surface immobilization efficiency a single biotin per antibody was desired and therefore a UV energy of 1.0 J/cm^2 was selected, with an average of 1.23 ± 0.02 conjugations per antibody. Since the antibody biotinylation occurs site-specifically and there are only two NBS sites that conjugation can occur at, we estimate that >90% of the IgG^{PSA} possesses at least a single biotin conjugation at an average of 1.23 biotins per antibody. No crosslinking was observed in the absence of IBA or in the absence of UV energy.

3.4. Determination of the photocrosslinking site by western blot analysis

To verify the specificity of IBA for the NBS site on IgG^{PSA} a western blot analysis was carried out with IBA–EG_{11}–Biotin photocrosslinked antibody under reducing conditions. The HRP–streptavidin probed film established that biotinylation occurred selectively to the antibody light chain, with the yield of conjugation being dependent on the amount of UV energy exposure (Fig. 3B). This result was consistent across all other antibodies that have been tested (Alves et al., 2012). The IgG^{PSA} antibody was also evaluated by dynamic light scattering post 1.5 J/cm^2 UV exposure to verify that UV exposure did not cause inter-antibody crosslinking or effect the global antibody structure (Supporting information Fig. S4).

3.5. Antibody immobilization efficiency

Having determined the optimal UV biotinylation conditions for IgG^{PSA} we then compared the UV-NBS^{Biotin} site-specific immobilization method to three other commonly employed antibody immobilization techniques: NHS–Biotin, lysine side chain immobilization (ε-NH_3^+), and physical adsorption. Utilizing the NHS–Biotin procedure provided by the manufacturer IgG^{PSA} was biotinylated with an average of 2.63 biotins per antibody, as determined by comparison of the UV-NBS^{Biotin} biotinylated IgG^{PSA} at 1 J/cm^2 UV energy to the NHS–Biotinylated IgG^{PSA} via an ELISA assay (Supporting information Fig. S5). The NHS–Biotin, ε-NH_3^+ and physical adsorption immobilization techniques result in highly disordered antibody immobilization through biotinylation or surface conjugation at random lysine side chains or weak non-specific hydrophobic surface interactions. We compared these three commonly used non-site-specific immobilization techniques to the UV-NBS^{Biotin} method for antibody immobilization efficiency, antigen detection sensitivity of the functionalized surface, LOD and dynamic antigen detection range.

96-well plates were functionalized using the four respective methods with initial antibody amounts ranging from 0 to 50 fmole (0–0.5 nM) of IgG^{PSA} to generate the antibody coated surfaces.

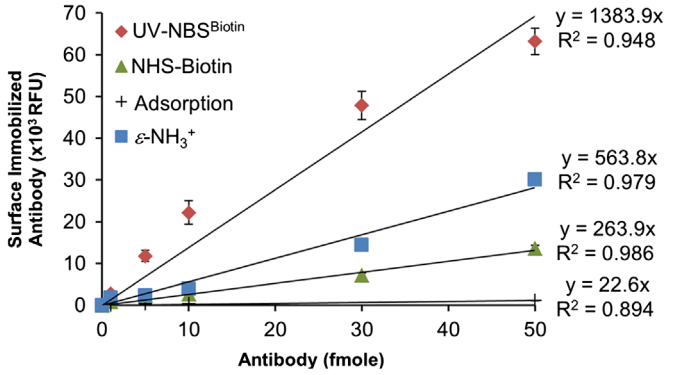

Fig. 4. Antibody immobilization efficiency of the UV-NBS^{Biotin} method in comparison to NHS–Biotin, ε-NH_3^+ and physical adsorption methods using IgG^{PSA}/PSA (antibody/antigen) system. 96-well plates were functionalized with IgG^{PSA} using all four methods. Total surface immobilized antibody was quantified using an HRP linked anti-Fc secondary antibody. *X*-axis shows the starting amount of antibody used to generate the surface, 0–50 fmole (0–0.5 nM).

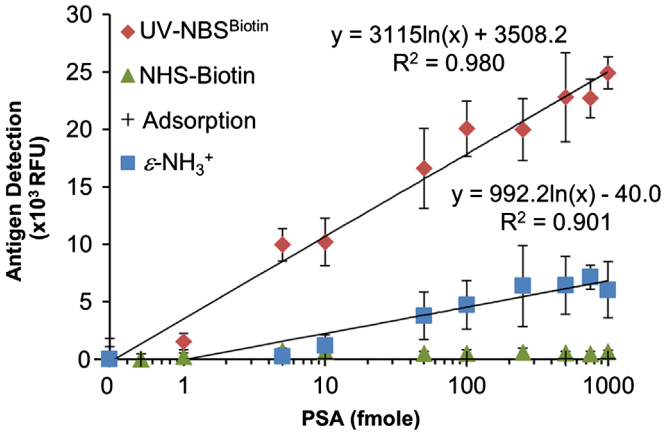

Fig. 5. Antigen detection intensities of the UV-NBS^{Biotin} method in comparison to NHS–Biotin, ε-NH_3^+ and physical adsorption methods using IgG^{PSA}/PSA (antibody/antigen) system. 96-well plates were functionalized with IgG^{PSA} (5 fmole, 0.05 nM) using all four methods. Antigen detection sensitivity was determined using increasing concentrations of PSA, 0–1000 fmole (0–10 nM) as the antigen, det-IgG^{PSA} and quantified by an HRP linked anti-Fc antibody as the reporter. Data represents means ($\pm$SD) of triplicate experiments.

The amount of surface immobilized antibody was then determined by binding of an HRP conjugated Fc-specific secondary antibody to the immobilized IgG^{PSA} capture antibody. The immobilization efficiency of IgG^{PSA}, determined by the slope of the antibody immobilization curve, using the UV-NBS^{Biotin} method demonstrated a 2.45, 5.24, and 61.12 fold enhancement in antibody immobilization when compared to the ε-NH_3^+, NHS–Biotin and physical adsorption methods, respectively (Fig. 4). These results demonstrate that the UV-NBS^{Biotin} method provides an effective antibody immobilization technique to generate the highest level of antibody functionalized surfaces.

3.6. Determination of antigen detection capabilities and assay sensitivity

Antigen detection and assay sensitivity for the antibody coated surfaces from each of the immobilization methods was also assessed. Assay sensitivity (*S*) is typically determined by the slope of the linear regression line obtained by plotting detection signal versus antigen concentration (Han et al., 2010). The assay sensitivity was calculated and compared for all four immobilization techniques using 5 fmole (0.05 nM) of initial IgG^{PSA} as the capture antibody, free PSA as antigen, det-IgG^{PSA} and an Fc-specific HRP conjugated antibody as the reporter. A fluorescent HRP substrate was employed to determine the antigen-response curve of a range of standard antigen concentrations from 0 to 1000 fmole (0–10 nM). These PSA antigen levels were below the limit of detection for the physical adsorption, and NHS–Biotin immobilization methods. The UV-NBS^{Biotin} immobilization method displayed the highest antigen detection intensities with the highest assay sensitivity (S=3,115.0, R^2=0.980) and the ε-NH_3^+ immobilization method demonstrated significantly lower antigen detection intensities with a lower sensitivity (S=992.2, R^2=0.901) (Fig. 5). From another perspective, surfaces generated using only 1 fmole (0.01 nM) of antibody via the UV-NBS^{Biotin} method delivered comparable antigen detection sensitivity (S=652.9, R^2=0.960) when compared to surfaces generated using 5 fold more antibody via the ε-NH_3^+ method (Supporting information Fig. S6). No antigen detection was observed with 1 fmole (0.01 nM) of starting antibody utilizing the ε-NH_3^+ immobilization method. The difference in assay sensitivity can best be explained by the enhanced binding efficiency of the UV-NBS^{Biotin} surface, resulting from improved immobilization of active antibody. Combined, these results demonstrate that surfaces generated by the UV-NBS^{Biotin} method produced a 3.14 fold higher sensitivity in antigen detection than the ε-NH_3^+ method.

3.7. Determination of the limit of detection (LOD) and dynamic antigen detection range

The exceptional antibody immobilization efficiency achieved with the UV-NBS^{Biotin} method provided enhanced sensitivity and a significant improvement to the limit of detection of PSA (3SD to the mean of the zero standard) compared to the ε-NH_3^+ immobilization method (Han et al., 2010). The LOD for the UV-NBS^{Biotin} method at starting antibody amounts of 1 and 5 fmole (0.01 and 0.05 nM) were comparable at 1.97 and 1.88 fmole of PSA (~0.02 nM), respectively. These LOD values signify a 15.63 fold reduction in the LOD of PSA when compared to the ε-NH_3^+ LOD of 29.36 fmole (0.29 nM) with 5 fmole (0.05 nM) of initial IgG^{PSA}. The UV-NBS^{Biotin} immobilization technique also demonstrated a 4.52 fold broader dynamic detection range for PSA, 1.88–1000 fmole (0.019–10 nM), compared to the ε-NH_3^+ detection range of 29.36–250 fmole (0.29–2.5 nM).

4. Conclusions

By site-specifically conjugating a biotin to the NBS of IgG^{PSA} prior to immobilization (UV-NBS^{Biotin} method) the low antibody immobilization efficiency associated with the previously described UV-NBS method was overcome by ensuring an average of ~1 biotin conjugation per antibody while still maintaining the highest level of antibody activity (Alves et al., 2012). Surfaces functionalized by the UV-NBS^{Biotin} method displayed significantly enhanced antibody immobilization efficiency, heightened antigen detection sensitivity, reduced LOD, and improved dynamic antigen detection range resulting in an overall increase in assay sensitivity compared to other commonly used antibody immobilization methods. Due to the limited detection area on the ever shrinking medical diagnostic devices it is critical that every antibody immobilized on the detection surface is capable of binding its intended antigen. With high crosslinking efficiencies, the UV-NBS^{Biotin} method provides for a site-specific covalent conjugation method that does not impact antigen or Fc binding interactions. By site-specifically conjugating a biotin molecule to antibodies, oriented immobilization can be carried out on any surface that bears streptavidin, regardless of antigen specificity. Taken together, the UV-NBS^{Biotin} method provides a universal, site-specific immobilization method that is amenable to any available assay detection modality with

potential significant implications in the development of miniaturized medical diagnostics and lab on a chip technologies.

Acknowledgments

The authors thank the Center for Environmental Science and Technology for usage of the DLS and the Notre Dame Mass Spectrometry and Proteomics Facility for usage of mass analysis instrumentation.

Appendix A. Supporting information

Supplementary data associated with this article can be found in the online version at http://dx.doi.org/10.1016/j.bios.2013.05.052.

References

Alves, N.J., Kiziltepe, T., Bilgicer, B., 2012. Langmuir 28, 9640–9648.
Alves, N.J., Champion, M.M., Stefanick, J.F., Handlogten, M.W., Moustakas, D.T., Shi, Y., Shaw, B.F., Navari, R.M., Kiziltepe, T., Bilgicer, B., 2013. Biomaterials 34, 5700–5710.
Brogan, K.L., Wolfe, K.N., Jones, P.A., Schoenfisch, M.H., 2003. Analytica Chimica Acta 496, 73–80.
Butler, J.E., Ni, L., Nessler, R., Joshi, K.S., Suter, M., Rosenberg, B., Chang, J., Brown, W. R., Cantarero, L.A., 1992. Journal of Immunological Methods 150, 77–90.
Butler, J.E., Ni, L., Brown, W.R., Joshi, K.S., Chang, J., Rosenberg, B., Voss Jr., E.W., 1993. Molecular Immunology 30, 1165–1175.
Byeon, J., Limpoco, F.T., Bailey, R.C., 2010. Langmuir 26, 15430–15435.
Caygill, R.L., Blair, G.E., Millner, P.A., 2010. Analytica Chimica Acta 681, 8–15.
Faye, C., Chamieh, J., Moreau, T., Granier, F., Faure, K., Dugas, V., Demesmay, C., Vandenabeele-Trambouze, O., 2012. Analytical Biochemistry 420, 147–154.
Ghani, R., Iqbal, A., Akhtar, N., Mahmood, A., Malik, N.S., Usman, M., Ali, H., Akram, M., Asif, H.M., 2011. Journal of Medicinal Plants Research 5, 2572–2576.
Han, H.J., Kannan, R.M., Wang, S., Mao, G., Kusanovic, J.P., Romero, R., 2010. Advanced Functional Materials 20, 409–421.
Handlogten, M.W., Kiziltepe, T., Moustakas, D.T., Bilgicer, B., 2011. Chemistry and Biology 18, 1179–1188.
Hoffman, W.L., Oshannessy, D.J., 1988. Journal of Immunological Methods 112, 113–120.
Hu, W., Li, C.M., 2011. Wiley Interdisciplinary Reviews: Nanomedicine and Nanobiotechnology 3, 119–133.
Kausaite-Minkstimiene, A., Ramanaviciene, A., Kirlyte, J., Ramanavicius, A., 2010. Analytical Chemistry 82, 6401–6408.
Kim, J., Yeo, W., Shu, Z., Soelberg, S.D., Inoue, S., Kalyanasundaram, D., Ludwig, J., Furlong, C.E., Riley, J.J., Weigel, K.M., Cangelosi, G.A., Oh, K., Lee, K., Gao, D., Chung, J., 2012. Lab on a Chip. 12, 1437–1440.
Lee, W., Oh, B., Lee, W., Choi, J., 2005. Colloids and Surfaces B: Biointerfaces 40, 143–148.
Lefranc, M.P., Pommie, C., Ruiz, M., Giudicelli, V., Foulquier, E., Truong, L., Thouvenin-Contet, V., Lefranc, G., 2003. Developmental and Comparative Immunology 27, 55–77.
Leonard, P., Hearty, S., Brennan, J., Dunne, L., Quinn, J., Chakraborty, T., O'Kennedy, R., 2003. Enzyme and Microbial Technology 32, 3–13.
Li, X., Conklin, L., Alex, P., 2008. World Journal of Gastroenterology 14, 5115–5124.
Liu, S., Zhang, X., Wu, Y., Tu, Y., He, L., 2008. Clinica Chimica Acta 395, 51–56.
MacBeath, G., Schreiber, S., 2000. Science 289, 1760–1763.
Meisenheimer, K.M., Koch, T.H., 1997. Critical Reviews in Biochemistry and Molecular Biology 32, 101–140.
Mendoza, L.G., McQuary, P., Mongan, A., Gangadharan, R., Brignac, S., Eggers, M., 1999. BioTechniques 27, 778.
Moelans, C.B., de Weger, R.A., Van der Wall, E., van Diest, P.J., 2011. Critical Reviews in Oncology Hematology. 80, 380–392.
Mohammed, M., Desmulliez, M.P.Y., 2011. Lab on a Chip. 11, 569–595.
Moyer, V.A., US Preventive Serv Task Force, 2012. Annals of Internal Medicine 157, 120.
Ng, A.H.C., Uddayasankar, U., Wheeler, A.R., 2010. Analytical and Bioanalytical Chemistry 397, 991–1007.
Patel, N., Davies, M.C., Hartshorne, M., Heaton, R.J., Roberts, C.J., Tendler, S.J.B., Williams, P.M., 1997. Langmuir 13, 6485–6490.
Peluso, P., Wilson, D., Do, D., Tran, H., Venkatasubbaiah, M., Quincy, D., Heidecker, B., Poindexter, K., Tolani, N., Phelan, M., Witte, K., Jung, L., Wagner, P., Nock, S., 2003. Analytical Biochemistry 312, 113–124.
Quarles, R.H., 1985. Journal of Applied Biochemistry 7, 347–355.
Rajagopalan, K., Pavlinkova, G., Levy, S., Pokkuluri, P.R., Schiffer, M., Haley, B.E., Kohler, H., 1996. Proceedings of the National Academy of Sciences USA 93, 6019–6024.
Shephard, G.S., 2008. Chemical Society Reviews 37, 2468–2477.
Sutcliffe, S., Pakpahan, R., Sokoll, L.J., Elliott, D.J., Nevin, R.L., Cersovsky, S.B., Walsh, P.C., Platz, E.A., 2012. BJU International 110, 1627–1635.
Trilling, A.K., Beekwilder, J., Zuilhof, H., 2013. Analyst 138, 1619–1627.
Vijayendran, R.A., Leckband, D.E., 2001. Analytical Chemistry 73, 471–480.
Vikholm-Lundin, I., 2005. Langmuir 21, 6473–6477.
Warsinke, A., 2009. Analytical and Bioanalytical Chemistry 393, 1393–1405.
Washburn, A.L., Gomez, J., Bailey, R.C., 2011. Analytical Chemistry 83, 3572–3580.
Xiong, Q., Ge, F., 2011. Expert Review of Proteomics. 8, 439–442.
Yotsumoto, H., 2008. Rinsho Byori 56, 1026–1033.
Zara, J.J., Wood, R.D., Boon, P., Kim, C.H., Pomato, N., Bredehorst, R., Vogel, C.W., 1991. Analytical Biochemistry 194, 156–162.